Limited sensitivity of published InSight RISE rotation products to the seismically proposed Martian inner-core family: a prospectively specified reanalysis

Artus Krohn-Grimberghe

Percivio Ltd.
Corresponding author: artus@percivio.com
ORCID: 0009-0001-4384-8306

Preprint statement. This manuscript is a non-peer-reviewed preprint submitted to EarthArXiv. It has not yet been submitted to a journal at the time of posting; submission to *Geophysical Journal International* is planned.

Data and code availability. The published inputs are public (the Le Maistre et al. 2023 SI fixed-period scan summary and source-data CSV, and the Bi et al. 2025 published values). Analysis code, the registered analysis plans and their amendment logs, registered input values, run manifests, and the interpretation records are archived as a versioned public deposit at https://doi.org/10.5281/zenodo.22127013.

Limited sensitivity of published InSight RISE rotation products to the seismically proposed Martian inner-core family: a prospectively specified reanalysis

Artus Krohn-Grimberghe — Percivio Ltd.

Corresponding author: artus@percivio.com. ORCID: 0009-0001-4384-8306.

Abstract

The InSight Rotation and Interior Structure Experiment (RISE) measured the rotation of Mars by radio tracking; Le Maistre et al. (2023) report the detection of the Free Core Nutation (FCN, period −243 ± 3.3 d) and no detection of the Free Inner Core Nutation (FICN) that a solid inner core would add. Bi et al. (2025) subsequently reported a 613 ± 67 km solid inner core from seismology, without addressing the FICN. We ask whether the published RISE rotation products can test that specific proposed core family — whether the FICN non-detection is evidential or uninformative — using three analyses whose grids, statistics, thresholds and outcome wordings were specified and archived before the outcome-determining computations were run. Analysis A, a forward detectability sweep over a registered 45-cell family grid (three radii × five density contrasts × three coupling treatments), evaluates 27 cells and conservatively withholds 18 under registered validity gates; every evaluated cell returns the registered verdict "below the measurement floor" from a joint consistency statistic against the published Mars-orientation uncertainties (largest per-cell reduced χ^2 0.2921; largest single-term diagnostic 2.105 σ). Analysis B projects the same family onto the published fixed-period FICN-strength scan and returns its registered outcome: "No evaluated admitted model has a FICN signature that is both representable in the published F* parameterization and demonstrably recoverable at the registered sensitivity. The published RISE FICN null is therefore uninformative for this test and supports neither the presence nor the absence of a Martian inner core." Analysis C, a joint Bayesian confrontation of inner-core radius and density contrast with the 16 published nutation-term perturbations, finds the family consistent with the published products (minimum joint χ^2 = 0.021) and the result prior-dominated:

the joint core posterior is the published seismic posterior essentially unchanged (90% width ratios 0.884 and 0.926). The inferred FICN period, residue, phase and damping depend on an Earth-anchored first-order gravitational-coupling treatment, zero-defaulted Mars compliances and the explicitly sampled coupling branches. Models outside those branches were not tested and are not excluded. At current sensitivity the published rotation products neither confirm nor refute the proposed inner core; we quantify the sensitivity gap and identify the observation types that could close it.

Keywords: Planetary interiors; Earth rotation variations; Composition and structure of the core; Inverse theory; Statistical methods.

1. Introduction

The InSight RISE radio-tracking experiment (Folkner et al. 2018) measured Mars' rotation and detected the Free Core Nutation, confirming a liquid core (radius ≈ 1,835 km; Le Maistre et al. 2023). A planet with a solid inner core inside that liquid core supports one additional rotational normal mode, the Free Inner Core Nutation (FICN). The FICN was not detected. Rivoldini et al. (2022) argued from core density that an inner core is "highly unlikely" and noted that a solid inner core "would lead to an additional rotational normal mode the signature of which has not been detected in the RISE data." Bi et al. (2025) then reported a 613 ± 67 km solid inner core (85% confidence interval; endpoints 546–680 km) from seismological analysis, without engaging the FICN question.

That an inner core should leave a rotational fingerprint on Mars was quantified well before InSight. Van Hoolst et al. (2000) characterized the free rotational modes of Mars interior models, and Defraigne et al. (2003) computed the FICN resonance for models with solid inner cores and examined its signature in the nutations as a function of interior structure; Baland et al. (2020) supply the rigid-Mars nutation baseline adopted by the RISE analysis. What none of these studies could use — because it did not yet exist — is a measured FCN, measured per-term nutation uncertainties, a published FICN-strength scan, and, decisively, a specific seismically proposed inner-core family to test. The seismic claim and the rotational non-detection have not previously been confronted quantitatively.

We quantify that previously unresolved cross-check: for the Bi et al. core family (radius, and plausible inner-core-boundary density contrasts), are the predicted rotational signatures above or below the published RISE measurement uncertainties — is the non-detection evidential, or uninformative? Three analyses address the question at increasing depth: Analysis A, a forward detectability sweep of the family against the published per-term uncertainties; Analysis B, a reanalysis of the published fixed-period FICN-strength scan asking whether the family's FICN signature is even representable and recoverable in that published search; and Analysis C, a joint Bayesian confrontation of the family with the published nutation-term products. Figure 1 summarizes the flow.

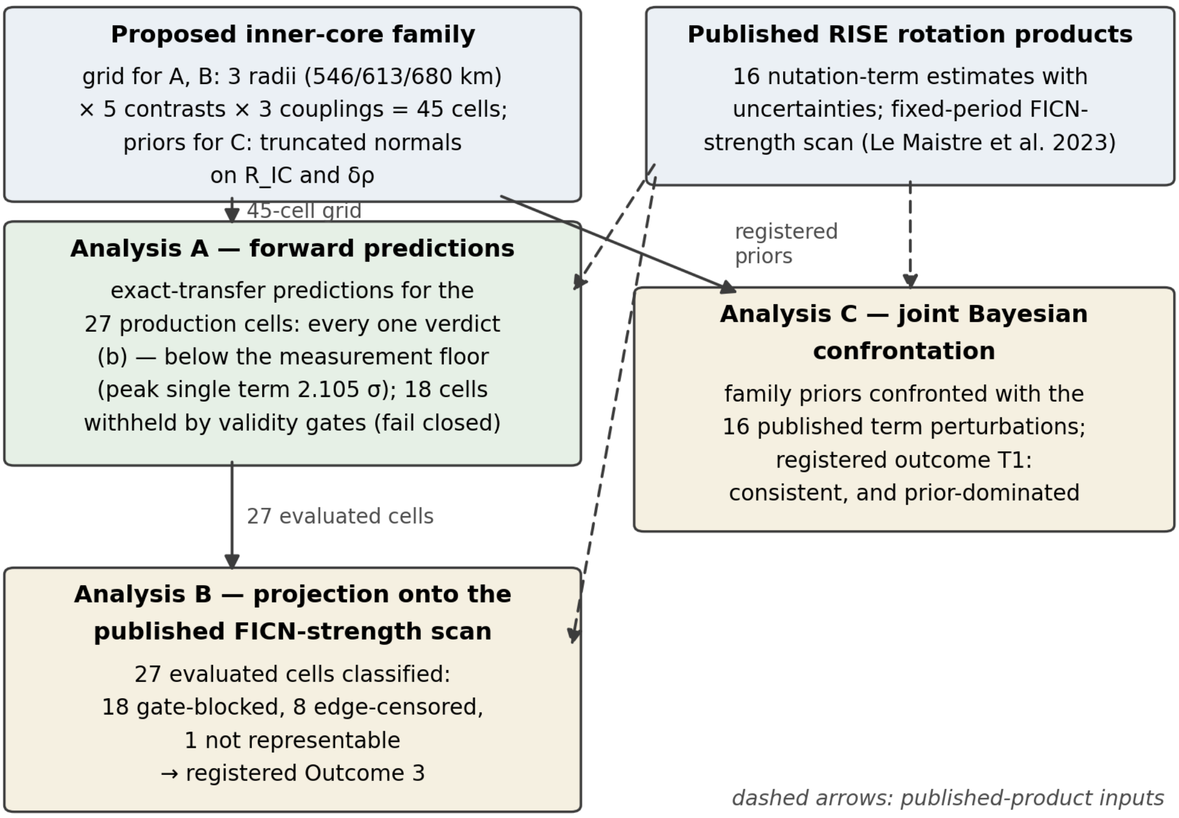

Figure 1. Flow of the three analyses. The registered 45-cell family grid (three radii × five density contrasts × three coupling treatments) enters Analysis A, which evaluates 27 production cells —

every one returning verdict (b), below the measurement floor — and conservatively withholds 18 under registered validity gates. Analysis B classifies the 27 evaluated cells against the published fixed-period FICN-strength scan (18 gate-blocked, 8 edge-censored, 1 not representable: the registered Outcome 3). Analysis C confronts the family with the 16 published nutation-term perturbations (registered outcome T1: consistent, and prior-dominated).

Alt text: Flow diagram. Two input boxes — the proposed inner-core family (a 45-cell grid and continuous priors) and the published RISE rotation products — feed three analysis boxes. Analysis A evaluates 27 production cells, all below the measurement floor, with 18 withheld by validity gates. Analysis B classifies the 27 evaluated cells as 18 gate-blocked, 8 edge-censored and 1 not representable, the registered Outcome 3. Analysis C returns the registered outcome T1: consistent, and prior-dominated.

The analysis choices — grids, statistics, thresholds, validity gates, and the verbatim wording of every possible outcome — were specified and archived in advance of the outcome-determining computations (Section 7 identifies the archived registration documents). One aspect of the time-line is disclosed prominently rather than buried: an exploratory proxy comparison (2026-07-06, archived) had already indicated the qualitative outcome before the analysis plans were registered. That comparison scaled a crude predicted FICN strength (leading-order rigid moment fraction) against the published $F^* = 4\times10^{-5} \pm 0.007$, finding margins of 0.0313 / 0.0558 / 0.0936 at 546 / 613 / 680 km — a predicted strength roughly 11–32× below the published uncertainty. The registered analyses reported here were therefore specified in documented knowledge of that old qualitative outcome and before any new exact-transfer output existed. They are prospectively specified reanalyses of a known confrontation under statistical reductions fixed in advance — not first outcome-blind confrontations — and the registration documents disclose this provenance. What prospective specification protects here is the statistical reduction itself: the outcome classes, their wording, and every threshold were fixed before the quantitative results that they classify existed.

Under the registered prominence rule, an uninformative non-detection must be reported as prominently as a tension-raising outcome would have been, and that commitment binds this manuscript: the headline result of all three analyses is that the published data cannot yet test the seismic claim.

2. Published inputs, the tested family, and notation

2.1 Published rotation products

Le Maistre et al. (2023) report Mars orientation parameters from ~2.5 years of InSight X-band Doppler tracking: nutation-term amplitudes with mas-scale uncertainties, the FCN period, and, in their supplementary information, a fixed-period FICN-strength scan with a conservative uncertainty summary: $F^* = 4\times10^{-5}$ with $\sigma = 0.007$, scanned over an a-priori window of 200–575 d, with simultaneous-fit FCN companions F = 0.052 ± 0.022 and T_FCN = −242.5 ± 11 d. Throughout this paper the published FICN-strength object is called the published fixed-period FICN-strength scan and conservative uncertainty summary (short: the fixed-period scan result); it is a scan summary, and the star in F^* labels the FICN-strength parameter, not complex conjugation.

2.2 The tested family

The tested family is a registered 45-cell grid over the Bi et al. core:

- **Radius** R_IC ∈ {546, 613, 680} km — the published 85% interval endpoints and central value.
- **Inner-core-boundary density contrast** $\delta\rho \in \{0, 0.02, 0.07, 0.12, 0.15\}$ (fractional). The axis spans the published amplitude-ratio inference of Bi et al. ($\delta\rho \approx 7 \pm 5\%$): 0.07 is the central value, 0.02 and 0.12 are the $\pm1\sigma$ values, 0 is the zero-contrast null, and 0.15 extends to composition-model values beyond the 1σ range. (The published velocity jump is $\delta Vp = 32 \pm 8\%$.)
- **Inner-core-boundary coupling** ∈ {0, ½, 1} × the Earth-anchored first-order gravitational-coupling value (MHB2002 Table 2), i.e. from uncoupled to the full Earth-anchored value.

Two registered branch axes accompany the grid. B1 is a sourced ±15% non-hydrostatic bound on the inner-core-boundary flattening. B2 varies the coupling damping along an **Earth-anchored diagnostic sensitivity axis**: multiplying one Earth-anchored complex coupling value by 0, ½, and 1. B2 is *not* a Martian coupling bracket — that one-dimensional segment does not span the physically relevant amplitude–phase space, no Mars-motivated viscomagnetic coupling range is fabricated, and every claim in this paper that touches B2 carries the subset-limited language of Section 5.

2.3 Notation

Symbol	Meaning
R_IC	inner-core radius (km)
$\delta\rho$	fractional density contrast across the inner-core boundary
δV_p	fractional P-wave velocity jump at the inner-core boundary (published seismic value)
FCN, FICN	Free Core Nutation; Free Inner Core Nutation. Negative periods denote retrograde motion.
−243 ± 3.3 d vs −242.5 ± 11 d	two published FCN-period values from two different estimators: the main RISE solution, and the companion fit of the fixed-period scan. They are not interchangeable and are never conflated here.
F*	published FICN-strength parameter of the fixed-period scan (the star is a label, not conjugation)
σ	the conservative uncertainty of the published scan summary (0.007)
σ_i	published per-term nutation amplitude uncertainty of term i (mas)
W	the a-priori FICN-period search window of the published scan, the closed interval [200, 575] d
T, T_twin	nutation transfer function of a family member and of its inner-core-free twin
ω_i	tidal frequency of nutation term i
$\eta_{rigid,i}$	published rigid-Mars amplitude of nutation term i (Baland et al. 2020)
δ_i	predicted perturbation of term i imprinted by the inner core (mas)
support(m)	the interval of FICN periods a family cell m can present to the published scan (Section 3.2)

3. Methods

All three analyses implement the published Sasao–Okubo–Saito / Mathews et al. rotational formalism for Mars (Sasao et al. 1980; Mathews et al. 1991; Van Hoolst et al. 2000; Defraigne et al. 2003; Baland et al. 2020; Dehant & Mathews 2015); the contribution is the registered confrontation of that formalism with the specific Bi et al. family and the measured RISE uncertainties, not new rotation theory. In the archived registration and run records the three analyses are named Layer 1, Layer 2, and Stage 2, respectively; this paper uses Analyses A, B, C throughout.

3.1 Analysis A: forward detectability

Analysis A computes, for every family cell, the predicted FICN period and the predicted perturbation δ_i of each of the 16 published nutation terms, and compares them with the published uncertainties under a registered three-outcome verdict rule: (a) published-consistency-tension candidate; (b) below the measurement floor; (c) coupling/contrast-constrained. The registered verdict is stated from a joint consistency statistic against the published Mars-orientation uncertainties — a χ^2 over the registered term set — with per-term mas and σ margins reported as diagnostics only: outcome (b) obtains when the joint statistic lies below the registered one-sigma-equivalent consistency region.

The perturbations use an exact twin-subtracted transfer, $\delta_i = (T - T\_twin)(\omega_i) \cdot \eta\_rigid,i$, evaluated by direct solve of the full angular-momentum state basis: each family member's transfer function minus that of its inner-core-free twin, evaluated at the frequency ω_i of term i and applied to the published rigid-Mars amplitudes. Before any Mars run, the implementation was required to reproduce Earth benchmarks: it matches the MHB2002 Table 3b FICN residue and the corresponding resonance-expansion mapping within 6.4%/0.44° and 5.7%/0.32° (amplitude/phase; registered tolerances 15%/15°).

Cells whose numerical results fail registered validity gates (adjacent-verdict stability; spectral sanity of the computed mode set) are conservatively withheld as untested rather than interpreted; Section 4.1 reports them.

3.2 Analysis B: reanalysis of the published fixed-period scan

The published fixed-period scan fits, at each candidate FICN period in W, a fixed-period FICN term to the RISE series, and summarizes the result as F* with a conservative uncertainty. Analysis B asks a precise question: does any family member imprint a signature that this published search could have represented and recovered? Its registered reduction:

1. **Projection.** Each cell's predicted response is projected onto the published scan's fitting template; the fit yields a best-fit real period and a template residual (the registration defines the fit rule in its § 4.3).
2. **Support.** For each cell m, support(m) is the closed interval hull of those best-fit real periods propagated through every registered branch — baseline, both flattening perturbations (B1±), and the damping treatments of the diagnostic axis (B2 × 0, ½, 1) — under the registered damping treatments of the projection. This hull is deliberately conservative: widening support(m) can move a cell toward the censored class below, but can never create a detection or an exclusion;

the registered boundary-equality convention acts in the direction that weakens any exclusion-class statement.

3. **Window membership.** support(m) is compared with the closed window W = [200, 575] d: a hull strictly inside W is eligible; a hull disjoint from W is out-of-window; any other configuration — including touching a boundary exactly — is classed as censored at the window edge.
4. **Representability.** An eligible cell must be expressible by the published template: its template residual must not exceed a registered tolerance (TOL-REP = 2×10^{-10}, set in advance at 100× the largest clean benchmark residual, rounded up). A cell that fails is "not representable": the published scan statistic is not the correct statistic for that predicted response — which is not evidence against the model.
5. **Recoverability.** A representable cell's predicted FICN strength is compared with the registered sensitivity of the published scan (signal-to-noise against the conservative uncertainty, with a registered detection threshold of 3.608); only then would consistency or tension with the published F* value be stated.
6. **Reduction.** A mechanical reducer maps the resulting per-cell states onto one of three registered outcome templates whose sentences were written in advance.

Numerical-validity gates (registered Tiers C/E/G) guard every step, and rows produced under damped projection mappings are census-disclosed diagnostics barred from named support under the registered precedence rule; quantifiers in every claim sentence range over exact-transfer evaluated cells only. The production run was followed by an independent re-execution on a second, independently maintained runner lineage, compared field-by-field by a pre-committed comparator: verdict EQUIVALENT, with zero inequalities of any class over all 270 rows.

3.3 Analysis C: joint Bayesian confrontation

Analysis C confronts the family with the published nutation-term products in a joint two-parameter posterior over (R_IC, δρ), with the coupling fixed at the Earth-anchored value and the flattening perturbation off.

Data and likelihood. The likelihood uses the 16 registered RISE nutation-term perturbations only. The published solution reports the nutation terms without an inner-core excess, so the registered observable convention sets the datum for each term perturbation to zero, with a per-term uncertainty derived from the published rigid-Mars amplitudes through the registered transfer contract (no direct per-term table of inner-core residuals is published). The working likelihood is diagonal Gaussian: $\ln L(\theta) = -\frac{1}{2}\,\chi^2\_\mathrm{joint}(\theta)$ with 32 degrees of freedom (real and imaginary parts of 16 terms). Published correlations and design cross-products are unavailable; Section 5 carries this limitation. $\chi^2\_\mathrm{joint}(\theta)$ therefore measures the size of the perturbations a family member θ would have imprinted, in units of the derived uncertainties.

Prior. The published seismic estimate is used directly: $R\_IC \sim N(613\ \mathrm{km}, 46.5\ \mathrm{km})$ truncated to [400, 800] km — the standard deviation converts the published 85% interval half-width (67 km) through the corresponding normal quantile — and $\delta\rho \sim N(0.07, 0.05)$ truncated to [0, 0.20], from the published amplitude-ratio inference. The confrontation thus asks: do the published rotation products reshape the published seismic posterior?

FCN treatment. The FCN period is excluded from the likelihood and recorded as a diagnostic only, for registered reasons: the absolute FCN period of the registered interior model reflects the parent (liquid-core) structure, not the inner core, so including it would test the parent model; and the published scan-companion FCN estimate belongs to a different estimator family than the main solution (Section 2.3). Section 4.4 reports the diagnostic.

Sampling and validation. The posterior is sampled by nested sampling (dynesty; Speagle 2020) with 500 live points to an evidence tolerance of 0.01. Before the single registered real-data fit, the machinery passed simulation-based calibration (Talts et al. 2018) at the production settings — 200 prior draws with registered rank-uniformity and central-interval coverage criteria — plus an injection-recovery control at a known family member. The registered consistency reference is one-sided: it asks whether even the best-fitting family member leaves a coherent excess, against $\chi^2_{0.99} = 53.486$ at 32 degrees of freedom; the registered adverse control verifies that a coherent two-standard-deviation displacement of all sixteen terms (expected statistic ≈ 96) is flagged by this reference. A registered contraction criterion (90% posterior-to-prior width ratio above 0.75 in both parameters) separates a prior-dominated outcome from a data-driven one, and the registered outcome templates carry pre-written sentences for each case.

4. Results

4.1 Analysis A: every evaluated cell is below the measurement floor

Of 45 cells, 27 production cells return verdict (b) and 18 cells fail closed — they are conservatively withheld as untested under the registered validity gates (15 adjacent-verdict-stability, 3 spectral-sanity); there are no (a) and no (c) production verdicts. The registered verdict statistic — the joint consistency χ^2 against the published uncertainties — lies deep inside the consistent region in every evaluated cell: the largest per-cell reduced χ^2 is 0.2921 (at 680 km). As per-term diagnostics, the peak single-term margins are 0.698 σ (546 km), 1.254 σ (613 km) and 2.105 σ (680 km); Figure 2 shows the per-term predicted perturbations against the published uncertainties for the three radii. A registered consistency control between the superseded proxy implementation (v4) and the exact transfer (v5) reports every production outcome unchanged, b $\longrightarrow$ b, with the joint statistic reduced in every production cell. Zeroing the Mars-defaulted compliances shifts the transfer ingredient by at most 6.33×10^{-2} across the 16 registered term frequencies — the recorded size of that approximation, far below the factor-scale movements separating verdict classes. Per the registered prominence rule, this outcome — geodesy cannot yet test the seismic claim — is the headline Analysis-A result, not a subsidiary caveat.

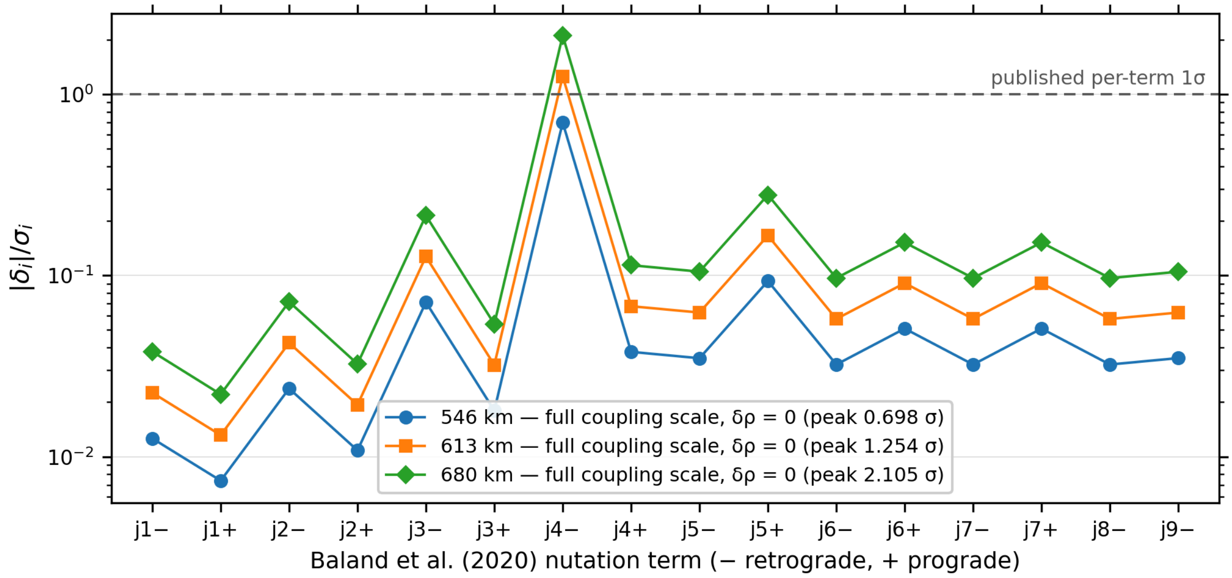

Figure 2. Predicted per-term nutation perturbations $|\delta_i|$ relative to the published per-term uncertainties σ_i, over the 16 registered nutation terms, for the maximum-response production cell at each family radius. The largest single-term diagnostics are 0.698 σ (546 km), 1.254 σ (613 km) and 2.105 σ (680 km); the registered verdict is stated from the joint statistic (Section 3.1), whose largest per-cell reduced χ^2 is 0.2921.

Alt text: Line plot on a logarithmic vertical axis showing the predicted perturbation of each of the 16 nutation terms divided by its published uncertainty, for the maximum-response cell at each of the three family radii. Most values lie between 0.01 and 0.3, below the dashed line marking one published standard deviation; a single term peaks at 0.698, 1.254 and 2.105 for the 546, 613 and 680 km radii, respectively.

4.2 Analysis B: the registered Outcome-3 result

The registered reducer, applied to the production run — clean at every global validity tier (no Tier G or Tier E gate fired; the Tier C numerical-validity gates G11 and G3 fired on 97 and 24 cell-branch scopes, respectively) — returns the registered Outcome-3 template for every mandatory branch-set, with all named sets empty. The registered sentence, emitted verbatim by the reducer:

> "No evaluated admitted model has a FICN signature that is both representable in the published F* parameterization and demonstrably recoverable at the registered sensitivity.

The published RISE FICN null is therefore uninformative for this test and supports neither the presence nor the absence of a Martian inner core."

In plain terms: of the 27 evaluated cells, 18 are withheld by numerical gates, 8 have period support reaching the edge of the published search window (censored: the window cannot contain their propagated support), and 1 is not representable by the published fitting template at all. Not one cell presents a signature the published scan could both represent and recover; consistency or tension with the published F* value is therefore never reached. The full state census over all 45 cells × 6 branch-sets (270 rows; 135 of them damped-mapping diagnostics):

branch	withheld (gate holes)	gate-blocked	edge-censored	not representable
baseline	18	21	6	0
B1−	18	11	15	1
B1+	18	13	13	1
B2 × 0	18	18	8	1
B2 × ½	18	22	5	0
B2 × 1	18	21	6	0
all	**108**	**106**	**53**	**3**

Every other registered state (out-of-window, ambiguous projection, recoverable-consistent, recoverable-inconsistent, not-recoverable) has zero rows. The 108 withheld rows are the 18 Analysis-A fail-closed holes × 6 branch-sets; these cells are untested, and no interpolation across them is performed. The exact-transfer composition (27 rows = 27 production cells under the undamped branch-set) is 18 gate-blocked, 8 edge-censored, 1 not representable; the damped-mapping diagnostics (135 rows) compose as 88 / 45 / 2 in the same states. Among the 56 evaluated rows, the support hull touches the lower window boundary in 32 rows, both boundaries in 3, the upper in 18, and neither in 3; the 3 strict-interior rows proceed down the ladder and are not representable (template residual exceeding TOL-REP — again, not evidence against those models: the published scan statistic is not the correct statistic for their predicted responses).

Reading of the censored states. A hull endpoint at exactly 200.0 d is the lower edge of the registered fit grid; a fit cannot express a period outside it. The honest reading of every censored row is that the propagated support **reaches the window boundary**; outside W the family's F* signature is **undetermined (censored), not detected and not excluded**. Boundary contact is branch-spread-driven, not nominal-period-driven: the nominal FICN periods of the family (248–545 d) lie inside the window, with edge margins of 48 d (lower) and 30 d (upper). Figure 3 shows the per-cell support hulls against the window.

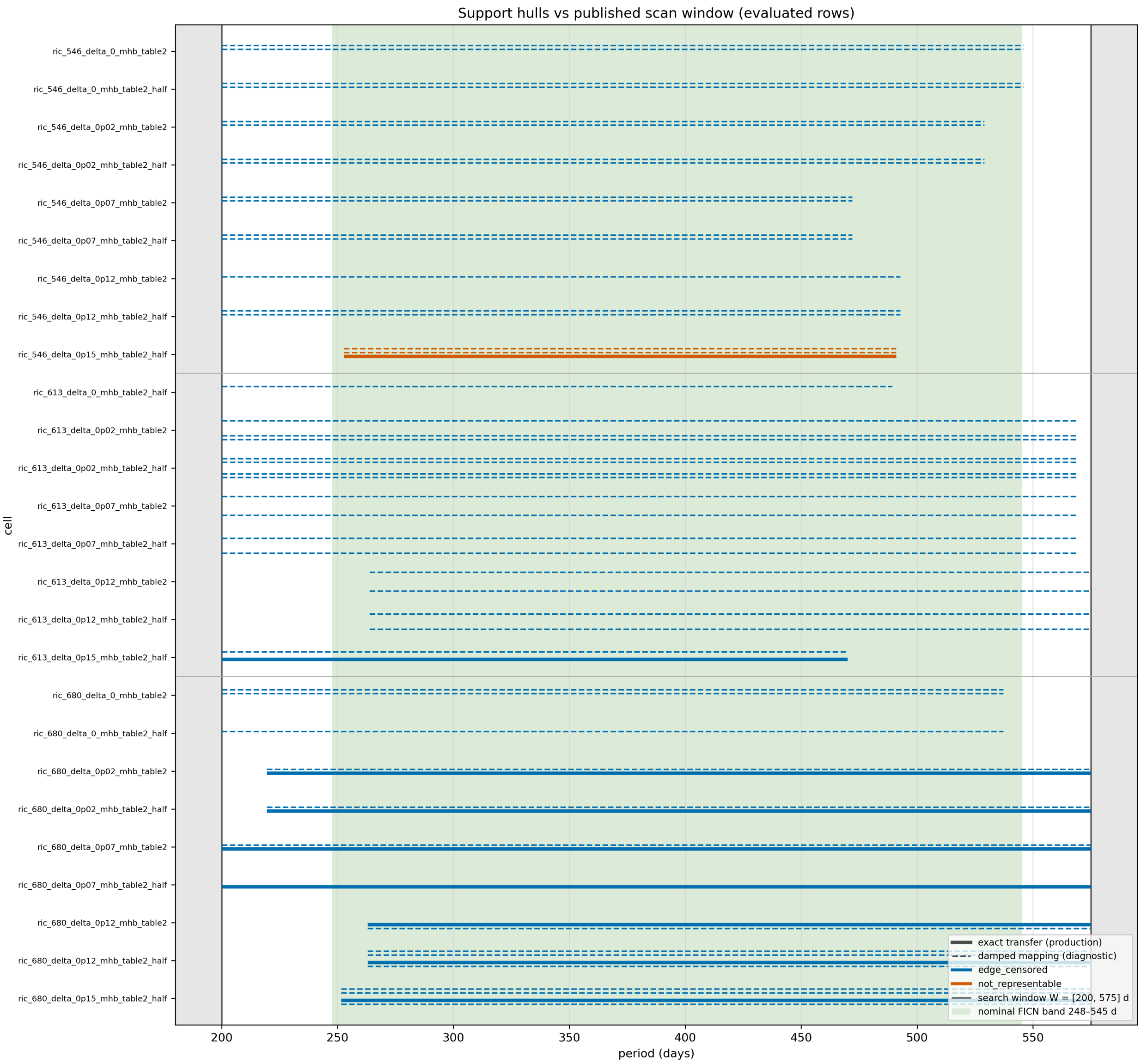

Figure 3. Per-cell period-support hulls of the evaluated family cells (horizontal bars) against the closed search window W = [200, 575] d of the published fixed-period FICN-strength scan, with the nominal FICN band 248–545 d shaded. Solid bars are exact-transfer production rows; dashed bars are damped-mapping diagnostic rows. Bars touching a window boundary are edge-censored:

outside W the family's F^* signature is undetermined (censored), not detected and not excluded. One row is not representable. The figure's registered caption, which fixes its claim scope, is archived verbatim in Supplement Section S5.

Alt text: Horizontal interval chart. Each evaluated family cell is one row; a horizontal bar spans that cell's support interval in period, plotted against the published search window from 200 to 575 days, with the nominal band from 248 to 545 days shaded. Solid bars are exact-transfer production rows and dashed bars are damped-mapping diagnostic rows. Nearly every bar reaches a window boundary (edge-censored); one row is marked not representable.

The claim scope of Figure 3 is fixed by its registered caption (archived verbatim in Supplement Section S5; the caption's "§ 4.3" denotes the fit-rule section of the archived registration, not a section of this paper): the plotted hulls are the closed interval hulls of the best-fit real periods under the registration's fit rule, propagated through the registered branches. B2 branches are an **Earth-anchored diagnostic sensitivity axis** (an Earth-anchored damping diagnostic), not a Martian coupling bracket, and no Martian-family uncertainty range is shown or implied. Quantifiers range over the evaluated exact-transfer subset only; damped rows are census-disclosed diagnostics; the 18 fail-closed holes are untested. The inferred FICN period, residue, phase and damping depend on an Earth-anchored first-order gravitational-coupling treatment, zero-defaulted Mars compliances and the explicitly sampled coupling branches. Models outside those branches were not tested and are not excluded.

Because 18 of the 27 exact-transfer production rows are gate-blocked, a natural question is whether the numerical gates could be hiding a detection. A registered descriptive census answers this counterfactually: re-applying the registered ladder through the window rung to the recorded per-cell support hulls of all 18 gate-blocked cells — i.e., assuming every Tier-C gate hypothetically cured — yields **18 of 18 `edge_censored`, 0 `interior — undetermined beyond window rung`, 0 `out_of_window`**. The one cell whose hull was previously unread (613 km, $\delta\rho = 0$, full coupling; hull [200.0, 489.25] d) is itself lower-boundary-touching. Under its registered positive control the same derivation reproduces the 9 evaluated rows' recorded composition, and its adverse control confirms a strict-interior hull would have been reported as such. This census is invariant to Tier-C gate-composition toggles holding each recorded per-cell support hull fixed; it does not establish invariance to a new numerical method or an altered frozen threshold that would recompute projections or hulls. Holding each recorded per-cell support hull fixed, no gate-composition toggle produces a recoverable exact-transfer state on the registered grid: the Outcome-3 composition is not an artifact of gate strictness.

A second question — prompted by critical review of an earlier draft, and answered by a disclosed post-registration census — is whether the diagnostic damping branches (B2 × ½, B2 × 1) materially set the recorded hulls, since an Earth-anchored diagnostic contributing hull endpoints could in principle drive the censoring. They do not. In none of the 27 recorded production hulls is an end-point attained *only* by a damped branch: every hull endpoint is also attained by undamped fits (the Supplement tabulates the per-cell attribution). Recomputing the hulls with the damped branch rows removed leaves the hull-level composition identical (26 censored, 1 not representable). A stricter zero-damping variant — which also drops the damped projection fits of the undamped branches — yields 2 censored and 25 not-representable cells: cells leave the censored class only by failing representability (template residuals near 10^{-2}, far above TOL-REP), never by becoming recoverable. The largest signal-to-noise ratio anywhere in the census is $\approx 2.7\times10^{-2}$, more than two orders of magnitude short of the registered recoverability threshold of 3.608 — so no hull geometry can reach a recoverable state. The registered Outcome-3 statement is unchanged under every variant. A positive control reproduced all 27 recorded hulls exactly, and adverse controls confirmed the census machinery reports strict-interior and recoverable states when present.

4.4 Analysis C: consistent, and prior-dominated

The fresh simulation-based calibration at the production settings passed every registered criterion: 200/200 draws; rank-uniformity p = 0.884 and 0.808 (R_IC, $\delta\rho$); 68% coverage 129/200 and 133/200 and 90% coverage 178/200 and 177/200, every Clopper–Pearson 95% interval containing its nominal level; contraction guard 0 violations across 200 draws; positive and adverse controls PASS. An injection-recovery control at θ_inj = (546 km, 0.02) recovered both injected values inside their 90% credible intervals. The single registered real-data fit (sampler seed 20260827, recorded in the archived record) then returned the registered outcome template T1, whose sentence is carried verbatim:

> "The registered fallback joint posterior is consistent with the published rotation data under the included-term diagonal statistic, and it is prior-dominated in both registered dimensions: the rotation data neither disfavour nor meaningfully sharpen the seismically proposed family in R_IC or in δρ. The joint core posterior is the published Bi posterior essentially unchanged; the seismic family survives the confrontation, and the geodetic contribution at current sensitivity is limited to the § 4-calibrated consistency statement."

(In the quoted registered sentence, "§ 4" denotes the calibration section of the archived production registration, not a section of this paper.) Here "rotation data" denotes only the 16 included nutation-term perturbations under the diagonal working likelihood; the FCN period, k_2 and the Phobos secular acceleration were not included.

Quantitatively: R_IC = 589 ± 41 km (90% credible interval [521, 657] km) and δρ = 0.077 ± 0.040 (90% CI [0.012, 0.141]), against the prior 613 ± 46.5 km and 0.07 ± 0.05. The posterior mean moves by 24 km in radius — about half a prior standard deviation — and by 0.007 in density contrast (about 0.14 prior standard deviations), while the 90% posterior-to-prior width ratios are 0.884 (R_IC) and 0.926 (δρ), both above the registered 0.75 contraction cut: the registered basis of the prior-dominated reading. Figure 4 overlays the posterior summaries on the prior densities.

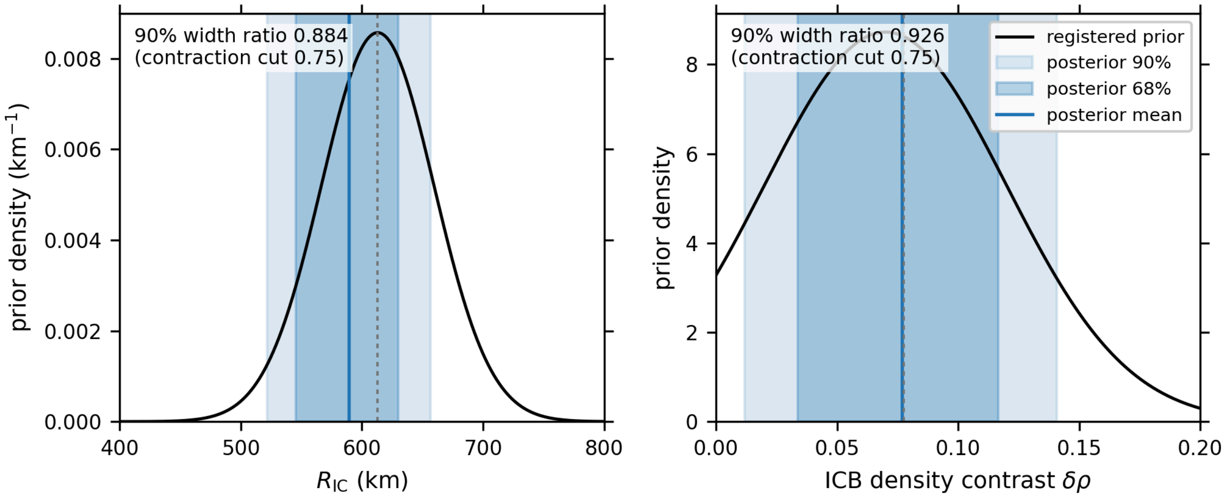

Figure 4. Analysis-C prior and posterior. Registered truncated-normal prior densities (Section 3.3) with the recorded posterior summaries (mean; 68% and 90% credible intervals) for R_IC (left) and δρ (right). The posterior is the prior essentially unchanged: 90% width ratios 0.884 and 0.926 against the registered 0.75 contraction cut.

Alt text: Two panels of prior density curves. The left panel shows the truncated-normal prior for the inner-core radius between 400 and 800 km; the right panel shows the prior for the boundary density contrast between 0 and 0.20. In each panel, shaded vertical bands mark the recorded 68% and 90% posterior credible intervals and a vertical line marks the posterior mean; the bands nearly fill the width of the prior, with 90% width ratios of 0.884 and 0.926.

The minimum joint χ^2 is 0.021 against the one-sided consistency reference $\chi^2_{0.99}$ = 53.486 at 32 degrees of freedom. A near-zero minimum is the expected signature of this regime, not an anomaly: because the registered data vector is the null perturbation (Section 3.3), χ^2_joint(θ) measures the perturbations a family member would have imprinted, and the smallest admitted members imprint almost nothing. The reference is calibrated to fire on a coherent excess — the registered adverse control confirms a two-standard-deviation coherent displacement of all sixteen terms (expected statistic ≈ 96) is flagged — and the observed statistic is deep in the consistent region.

The FCN diagnostic, recorded outside the likelihood: the registered interior model's FCN period at the family's central member is −222.0 d in the registered convention — an offset from the measured −243 ± 3.3 d that reflects the registered parent (liquid-core) structure, not the inner core. Across the joint posterior, the inner-core-induced shift of the FCN period is +0.43 ± 0.14 d — nearly an order of magnitude below the published uncertainty of the measured FCN period. Both facts support the registered exclusion of the FCN period from the likelihood: it constrains the parent model, not the tested inner-core family, at current sensitivity.

5. Discussion and limitations

Mandatory limitation statement (registered; carried verbatim on every claim-bearing surface of this analysis):

> "The inferred FICN period, residue, phase and damping depend on an Earth-anchored first-order gravitational-coupling treatment, zero-defaulted Mars compliances and the explicitly sampled coupling branches. Models outside those branches were not tested and are not excluded."

What the three analyses establish, and no more: at the published sensitivity, the RISE rotation data cannot test the Bi et al. inner-core family. The forward predictions sit deep inside the joint consistency region of the published uncertainties, with single-term diagnostics at most 2.105 σ (Analysis A); under the registered reduction of the published FICN-strength scan, no evaluated model is simultaneously representable and recoverable (Analysis B, Outcome 3); and the joint confrontation returns the published seismic posterior essentially unchanged (Analysis C, T1). The result is a failure of the registered sensitivity test: it is not evidence for the no-inner-core hypothesis and not evidence against any evaluated model; no cell is disfavoured or named; no continuous bound is inferred; the 18 holes stay untested.

Scope limitations, disclosed:

1. **Evaluated-subset ceiling.** All quantifiers range over evaluated exact-transfer cells (27 production cells; three discrete radii). No interpolation converts three radii into continuous-family coverage.
2. **B2 is diagnostic, not coverage.** The coupling-damping axis is Earth-anchored; the true Martian complex coupling is not established to lie on that segment. A Mars-motivated visco-magnetic coupling treatment is deferred work and is not fabricated here.
3. **Formalism level.** Earth-anchored first-order gravitational coupling and zero-defaulted Mars compliances (measured approximation size $\leq 6.33\times10^{-2}$ on the transfer ingredient); the claim domain is reduced accordingly rather than propagated as additional branches.
4. **Censoring, not absence.** Edge-censored rows mean the propagated support reaches the window boundary of the published scan; the family's F^* signature outside W is undetermined.
5. **Diagonal working likelihood.** Published correlations and design cross-products of the RISE solution are unavailable; Analysis C is a diagonal-statistic confrontation only, and its per-term uncertainties are derived quantities (Section 3.3), not a published inner-core residual table.
6. **The fuller joint inversion remains unexecuted.** Analysis C is the registered fallback likelihood: it omits the FCN period, k_2, and the Phobos secular acceleration. The anticipated fuller inversion — adding those constraints, ideally with the full covariance of a raw-Doppler re-estimation — has not been executed; no result exists for that combination.

What could close the sensitivity gap: longer radio-tracking baselines (the published products reflect ~2.5 years), a future geodetic lander, or a joint inversion of the raw Doppler records combining the nutation terms with the FCN period, k_2 and the Phobos secular acceleration under a full covariance model. Until then, rotational data neither confirm nor refute the seismically proposed inner core.

6. Conclusions

We asked whether the published InSight RISE rotation products can test the seismically proposed Martian inner-core family of Bi et al. (2025), using three analyses whose statistical reductions were specified and archived in advance.

They cannot, at current sensitivity — and that is the registered headline result, stated with its registered scope. Analysis A: all 27 evaluated family cells return the registered verdict "below the measurement floor" from the joint consistency statistic (largest per-cell reduced χ^2 0.2921; largest single-term diagnostic 2.105 σ); 18 further cells are withheld by validity gates and stay untested. Analysis B: the published fixed-period FICN-strength scan could not have represented and recovered any evaluated member's signature — "No evaluated admitted model has a FICN signature that is both representable in the published F* parameterization and demonstrably recoverable at the registered sensitivity. The published RISE FICN null is therefore uninformative for this test and supports neither the presence nor the absence of a Martian inner core." — and that composition is robust both to hypothetical curing of every numerical gate and to removal of the diagnostic damping branches from the support hulls. Analysis C: the joint core posterior is the published seismic posterior essentially unchanged (posterior 589 ± 41 km against prior 613 ± 46.5 km; 90% width ratios 0.884 and 0.926).

The non-detection of the FICN is therefore uninformative for this family: it neither confirms nor refutes the seismic claim. The registered limitation statement bounds every claim above; in particular, models outside the explicitly sampled branches were not tested and are not excluded. The sensitivity gap is quantified and specific — every evaluated forward prediction deep inside the joint consistency region of the published uncertainties, the published FICN-strength search unable to represent and recover any evaluated member's signature, and predicted FICN-period shifts nearly an order of magnitude below the FCN-period uncertainty — and identifies what a future geodetic measurement must deliver to turn this null into a test.

7. Data and code availability

"Raw Doppler and calibration records: public through PDS. Original GINS/MONTE software, production design matrices and normal equations: unavailable. A faithful raw-Doppler re-estimation is outside the registered scope and would require an independent observation-model implementation."

The published inputs are the Le Maistre et al. (2023) SI fixed-period scan summary and source-data CSV (transcription rows recorded before use) and the Bi et al. (2025) published values; Konopliv et al. (2020) values are cited as corroboration only. Analysis code, the registration documents and their amendment logs, registered input values, run manifests, and the interpretation records are archived in the project repository and its evidence store (Zenodo, DOI 10.5281/zenodo.22127013). The registration governing Analysis B was archived before execution; its SHA-256 checksum is `f47a49f0c17651f2e9d578e4fa115d32eea5c6f7ee0445f37f4be1e62c26c1ac`, and the checksums of every other governing record (registrations, run manifests, machine records, interpretation records) are listed in the Supplement, allowing readers to verify the archived files.

Acknowledgements

This work received no external funding. AI-assisted engineering and analysis were used throughout — Anthropic Claude and OpenAI GPT model families for code implementation, verification runs, literature retrieval and drafting support — under prospectively specified, human-controlled analysis plans; all scientific choices, registered statements and conclusions are the author's, and the author takes full responsibility for the content. The author thanks the InSight RISE and seismology teams, whose public data products made this reanalysis possible.

References

Baland, R.-M., Yseboodt, M., Le Maistre, S., Rivoldini, A., Van Hoolst, T. & Dehant, V. (2020). The precession and nutations of a rigid Mars. *Celestial Mechanics and Dynamical Astronomy* 132(9), 47. doi:10.1007/s10569-020-09986-0

Bi, H., Sun, D., Sun, N., Mao, Z., Dai, M. & Hemingway, D. (2025). Seismic detection of a 600-km solid inner core in Mars. *Nature* 645, 67–72. doi:10.1038/s41586-025-09361-9

Defraigne, P., Rivoldini, A., Van Hoolst, T. & Dehant, V. (2003). Mars nutation resonance due to Free Inner Core Nutation. *Journal of Geophysical Research: Planets* 108(E12), 5128. doi:10.1029/2003JE002145

Dehant, V. & Mathews, P. M. (2015). *Precession, Nutation and Wobble of the Earth.* Cambridge University Press. doi:10.1017/CBO9781316136133

Folkner, W. M., Dehant, V., Le Maistre, S., Yseboodt, M., Rivoldini, A., Van Hoolst, T., Asmar, S. W. & Golombek, M. P. (2018). The Rotation and Interior Structure Experiment on the InSight mission to Mars. *Space Science Reviews* 214, 100. doi:10.1007/s11214-018-0530-5

Konopliv, A. S., Park, R. S., Rivoldini, A., Baland, R.-M., Le Maistre, S., Van Hoolst, T., Yseboodt, M. & Dehant, V. (2020). Detection of the Chandler Wobble of Mars from orbiting spacecraft. *Geophysical Research Letters* 47, e2020GL090568. doi:10.1029/2020GL090568

Le Maistre, S., et al. (2023). Spin state and deep interior structure of Mars from InSight radio tracking. *Nature* 619, 733–737. doi:10.1038/s41586-023-06150-0

Mathews, P. M., Buffett, B. A., Herring, T. A. & Shapiro, I. I. (1991). Forced nutations of the Earth: influence of inner core dynamics: 1. Theory. *Journal of Geophysical Research: Solid Earth* 96(B5), 8219–8242. doi:10.1029/90JB01955

Mathews, P. M., Herring, T. A. & Buffett, B. A. (2002). Modeling of nutation and precession: new nutation series for nonrigid Earth and insights into the Earth's interior. *Journal of Geophysical Research: Solid Earth* 107(B4), 2068. doi:10.1029/2001JB000390

Rivoldini, A., Le Maistre, S., Caldiero, A., Yseboodt, M., Baland, R.-M., Beuthe, M., Van Hoolst, T., Dehant, V., Folkner, W., Buccino, D., Kahan, D., Marty, J.-C., Antonangeli, D., Badro, J., Drilleau, M., Konopliv, A., Peters, M.-J., Plesa, A.-C., Samuel, H., Tosi, N. & the InSight/RISE team (2022). A view into the deep interior of Mars from nutation measured by InSight RISE. *Europlanet Science Congress 2022*, EPSC2022-1101. doi:10.5194/epsc2022-1101

Sasao, T., Okubo, S. & Saito, M. (1980). A simple theory on the dynamical effects of a stratified fluid core upon nutational motion of the Earth. In: *Nutation and the Earth's Rotation* (IAU Symposium 78), 165–183. doi:10.1007/978-94-010-9568-6_27

Speagle, J. S. (2020). dynesty: a dynamic nested sampling package for estimating Bayesian posteriors and evidences. *Monthly Notices of the Royal Astronomical Society* 493(3), 3132–3158. doi:10.1093/mnras/staa278

Talts, S., Betancourt, M., Simpson, D., Vehtari, A. & Gelman, A. (2018). Validating Bayesian inference algorithms with simulation-based calibration. arXiv:1804.06788

Van Hoolst, T., Dehant, V. & Defraigne, P. (2000). Chandler wobble and Free Core Nutation for Mars. *Planetary and Space Science* 48, 1145–1151. doi:10.1016/S0032-0633(00)00099-4